Winter-time Hydraulic Jump over the Pokhara Valley, Nepal

S. Shrestha and R. P. Regmi

Journal of Nepal Physical Society

Volume 9, Issue 1, June 2023

ISSN: 2392-473X (Print), 2738-9537 (Online)

JNPS, **9** (1): 98-106 (2023)

DOI: https://doi.org/10.3126/jnphyssoc.v9i1.57739

Published by:

Nepal Physical Society
P.O. Box: 2934
Tri-Chandra Campus
Kathmandu, Nepal
Email: nps.editor@gmail.com

JNPS 9 (1): 98-106 (2023)
ISSN: 2392-473X (Print), 2738-9537 (Online)
Research Article *© Nepal Physical Society*
DOI: https://doi.org/10.3126/jnphyssoc.v9i1.57739

Winter-time Hydraulic Jump over the Pokhara Valley, Nepal

S. Shrestha[*] and R. P. Regmi
National Atmospheric Resource and Environmental Research Laboratory
Central Department of Physics, Tribhuvan University, Kirtipur, Nepal
* Corresponding Email: sajan.shrestha@narerl.tu.edu.np

Received: *2nd April, 2023;* ***Revised:*** *20th June, 2023;* ***Accepted:*** *28th June, 2023*

ABSTRACT

The Pokhara Valley is set to be one of the aviation hubs of Nepal with the opening of an international airport. The complex mid-hill mountainous topography of the Gangi-Himalaya and the characteristic wind system of the valley make safe aviation rather challenging over the valley. This study using the Weather Research and Forecasting modeling system shows that hydraulic jump-like phenomena occur regularly during winter in the western and central part of the Pokhara Valley during late afternoon/early evening when the airport may remain relatively busy. The jump occurs over the western part of the valley when the regional southwesterly plain to mountain wind via the Putalibazar Valley intrudes into the Valley crossing the Deurali-Mattikhan hill. The jump-like flow is accompanied by the formation of a mild reverse roller above the jump region and the head-on convergence with the northeasterly katabatic/drainage wind from Parche-Namarjung along the southeast–northwest oriented valley axis generating an updraft of as much as 0.4 to 0.8 m s^{-1}. The southwesterly overrides northeasterly generating clockwise vertical rotors and high turbulence over the northeastern region of the valley. An early prediction of possible wind hazards at high spatiotemporal resolutions are highly desired to make aviation activities in the region safer for civil aviation.

Keywords: Aviation wind hazard, Himalaya, Hydraulic jump, Pokhara valley, Pokhara international airport.

INTRODUCTION

On 1050 Local Standard Time (LST) - 15 January 2023, an ATR-72-212A aircraft of Yeti Airlines (call sign – NYT-691) flying from Kathmandu to Pokhara crashed at Seti River Gorge, 1800 m North-west of the Pokhara International Airport (PIA), killing all the 72 people onboard, while approaching to land [CAAN 2023a, 2023b]. The accident is one of the worst aviation disasters in the country and a big red flag to the national aviation safety record, particularly for the Pokhara Valley. The PIA is expected to be one of the busiest airports of the nation in the future with the inauguration of the newly opened international airport. Similarly, 17 people have lost their lives in paragliding accidents in the valley since 1996 [Himalisanchar 2022]. While the detailed role of meteorological conditions for the NYT-691 accident is yet to be investigated, and the role of prevailing weather may not be ignored, a deterministic role of weather can be acknowledged in the lighter aircraft accidents in the region. The need for understanding of detailed wind system over the complex terrains of the valley and possible wind hazards is necessary, considering the difficult topography and its interaction with synoptic and regional winds.

Atmosphere - Mountain (Topography) interaction generates a spectrum of atmospheric disturbances manifesting usually as terrain-enforced precipitation, slope winds, pass winds, downslope storms, mountain waves, hydraulic jumps, etc. [Whiteman 2000]. The prevailing atmospheric stability, wind speed, and topographic structure and orientation determine the nature, severity, and scale of such interaction. For example, hydraulic jump-like phenomena that have been frequently reported in the Kathmandu valley [Regmi *et al.* 2003, 2019] and Kali Gandaki valley [Regmi 2014], located in the Himalayan foothills, occur when a mean wind,

strong enough crosses a topographic barrier perpendicular to the wind in presence of stable atmosphere over the barrier.

The flow on the lee slope squeezes and accelerates downhill. On approaching the lee plain, the flow downstream makes sudden deceleration inflating the layer and creating a flow jump, called a hydraulic jump. The fluid layer depth discontinuity is accompanied by the dissipation of kinetic energy; thus, the area of the jump is highly turbulent and hazardous, and is accompanied by the occasional rotor and reverse roller formation [Rotunno and Bryan 2018]. Here the flow makes an abrupt and discontinuous transition from supercritical to subcritical flow characterized by a change of nondimensional parameter called Internal Froude number (Fr), i.e. the Fr changes from >1 (supercritical) to <1 (subcritical) in the lee plain. The Froude number is the ratio of wind speed to atmospheric stability and is mathematically represented in equation (1).

$$Fr = \frac{V}{\sqrt{\frac{\Delta\theta}{\theta}gh}} \quad \text{.......................................} (1)$$

In Equation 1, V is the mean wind speed of the layer, θ is the mean potential temperature, $\Delta\theta$ is the potential temperature difference between the layer top and bottom, g is the acceleration due to gravity, and h is the thickness of fluid/wind layer.

The occurrence of hydraulic jumps is a frequent phenomenon in the complex mountainous region e.g. Alaiz mountain range in Spain [Pena and Santos 2021], Taebeek Mountain in South Korea [Lee *et al.* 2020], Kathmandu valley [Regmi *et al.* 2003, 2019], Jomsom, etc. in the Himalayan mountain range [Regmi 2014], etc.

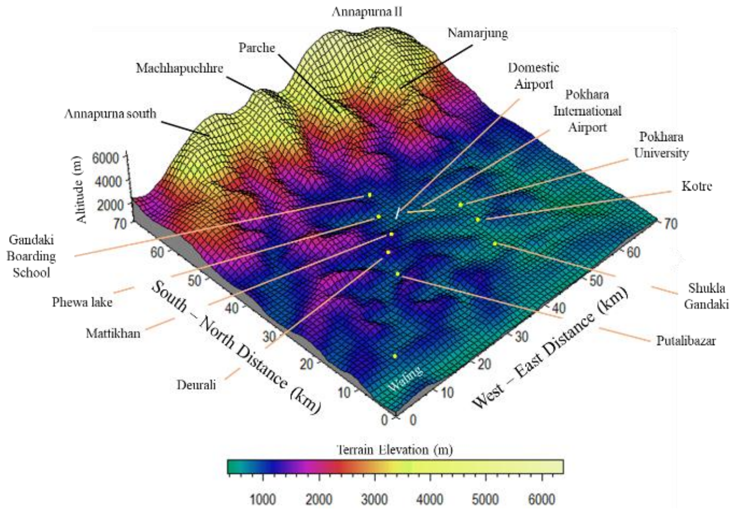

Fig. 1: Birds eye view of Pokhara valley and surrounding area. Important locations are mentioned in the figure.

The Pokhara Valley, situated in the mid-hills of western Nepal Himalaya, is a shallow elongated valley, 17 to 25 km long, aligned and sloped northwest (9 km width) to the southeast (2 km width) (see Figure 1). High mountain peaks like Machhapuchhre and Annapurna range forms the northern boundary of the valley, while shallow hill ranges bound east and south. Particularly the east-west aligned hill appears a suitable barrier to the regional southerly/south-westerly winds in the mid-hill region of Nepal that might result in the hydraulic jump under suitable conditions. As the Pokhara valley in its small space houses two airports, the hydraulic jumps and wind system could be critical for its air safety. In this study, we will present the hydraulic jump characteristic in the Pokhara Valley based on high-resolution numerical weather reconstruction.

MODEL SETUP AND DOMAIN CONFIGURATION

The state-of-the-art of the Advanced Research Weather Research Forecasting model (WRF-ARW) version 4.2.1 [Skamarock *et al.* 2019] was used for the reconstruction of the six-day (09 - 17 February 2021) wintertime weather of the Pokhara Valley and the surrounding region. The WRF is a non-hydrostatic atmospheric model suitably used for both the operational weather forecast and weather reconstructions. WRF has been successfully used at

high resolution in the Himalayan complex terrain of Nepal to study its atmospheric dynamics [Collier and Immerzeel 2015], extreme weather [Norris *et al.* 2015], aviation hazards [Regmi *et al.* 2020, 2017], air pollution dispersion [Kitada and Regmi 2003, Regmi *et al.* 2019, Panday *et al.* 2009, etc.], wind energy forecasting [Regmi and Maharjan 2013], etc.

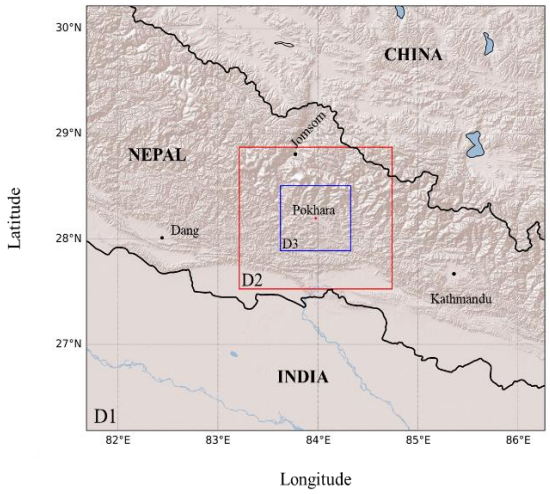

Fig. 2: Triply nested two-way interacting domain system configuration of the WRF simulation.

For this study, a triply nested two-way interacting domain system was set up (see Figure 2) all centered at the terminal of the domestic airport (28.12 °N, 83.98 °E) at the Pokhara valley. The finest domain (D3), fine domain (D2), and coarse domain (D1) consisted of 70 × 70, 51 × 51, and 51 × 51 horizontal grid points at 1 km × 1 km, 3 km × 3 km, and 9 km × 9 km horizontal resolution, respectively. There were 34 vertical grid points with the model top at 100 hPa. The parametrizations options consisted of the Dudhia scheme [Dudhia 1989] for shortwave radiation, the RRTM scheme [Mlawer *et al.* 1997] for long-wave radiation, the Thompson graupel scheme [Thompson *et al.* 2004] for cloud microphysics, MYJ scheme [Janjić, 2001] for the planetary boundary layer, and the Noah land-surface model [Chen and Dudhia, 2001].

The model was initialized with 1° × 1° horizontal resolution meteorological data from the operational analysis performed every 6 hours at the National Centers for Environmental Prediction. Similarly, in geostatic data, the 24-category land-use and 30-second terrain elevation data of the United States Geological Survey were used.

RESULTS AND DISCUSSION

In this section, we validate the model output with available observations and present the characteristics of near-surface winds, meteorological conditions triggering the hydraulic jump, and the jump characteristics during a typical clear-weather winter day over the Pokhara Valley.

Validation of Model output

For the validation of the WRF output, observation from the Automated Weather Station (AWS) at the Pokhara domestic airport maintained by the Department of Hydrology and meteorology, Government of Nepal has been used. The comparison of the diurnal variation of six-day air temperature and humidity at 2 m Above Ground Level (AGL) and wind speed and direction at 10 m AGL and their corresponding regressions are presented in Figure 3 (a-d) and 3(a'-d'), respectively.

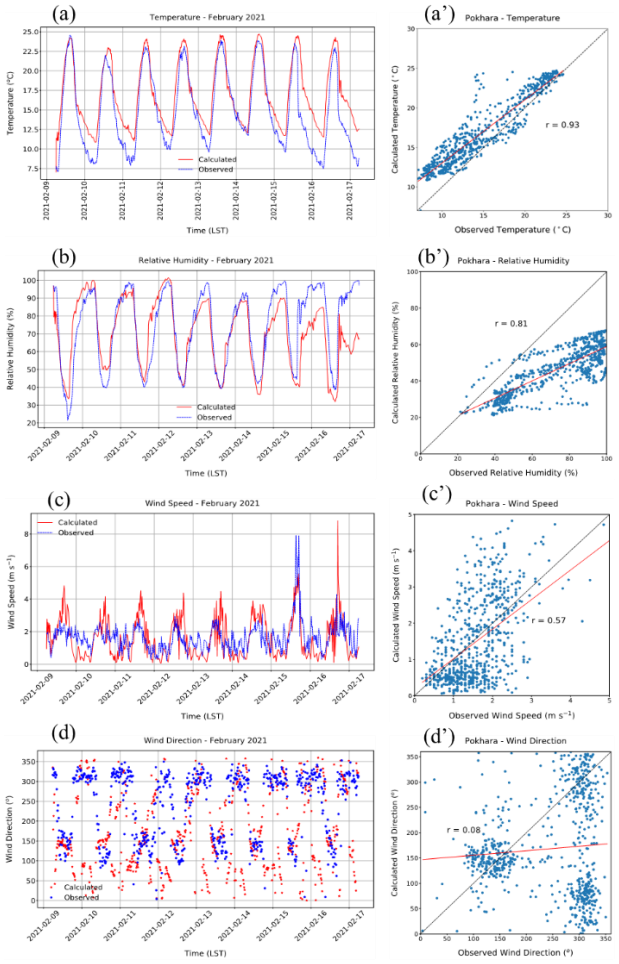

Fig. 3: Comparison of the WRF calculated and AWS recorded (a) temperature, (b) relative humidity, (c) wind speed and (d) wind direction. The corresponding scatter plot and the value of correlation coefficient are presented in 3(a' - d').

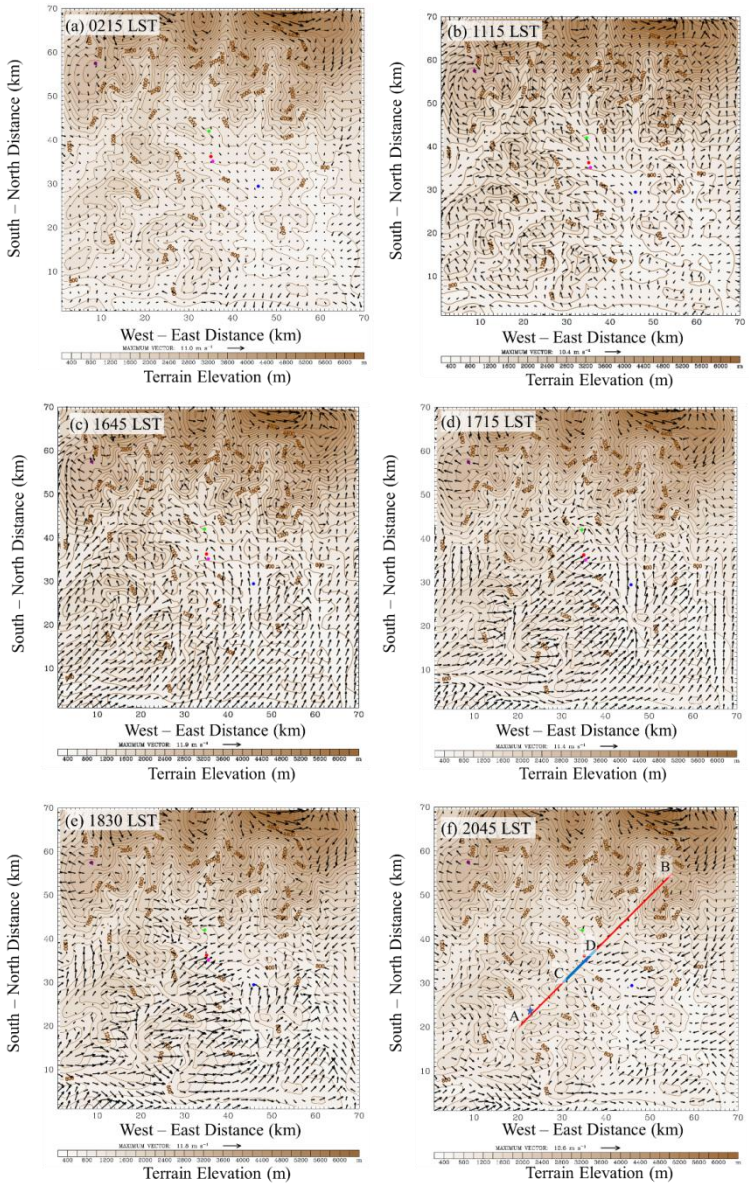

Fig. 4: Spatial distribution of near surface wind over the Pokhara Valley at selected times on 13 February 2021. Star symbol in Figure 4f represents the location of Putalibazar.

The comparisons show that all the parameters have been well reproduced with the correlation coefficient of 0.93 for temperature, 0.81 for humidity, 0.57 for wind speed, and 0.08 for wind direction. Considering the high variability of wind direction for low wind speed, especially in complex terrain like Pokhara, major wind directions of the valley appear to be captured well though the correlation statistics points otherwise.

The detailed inspection of the comparisons shows that the temperature seems overpredicted and humidity slightly under-predicted by the WRF during the night and early morning time. Similarly, wind speed is slightly over-predicted during the day and underpredicted during night and morning time. The day-to-day comparison suggests that temperature, humidity speed, and direction has been best reproduced during 13 and 14 February 2021. Thus, in this paper, necessary wind and hydraulic jump characteristics in the Pokhara Valley are discussed with reference to 13 February 2021.

Near-surface wind

The nighttime near-surface atmosphere of the Pokhara Valley appears calm and stable with mild down-valley winds of less than 1 m s^{-1} that make anti-clockwise circulation over the southeastern part of the valley (see Figure 4a for 0215 LST). The katabatic and down valley wind quickly appears

weak and disappears as it is not able to penetrate the near-surface layer due to the formation of the pool of cold air gaining nocturnal stability by the radiational cooling and accumulation of the down valley wind earlier.

The nocturnal stable layer remains shallow growing to around 50 m AGL at the domestic airport till 0815 LST. However, with the increased solar insolation after 0815 LST, the surface heating induces the upslope/anabatic wind in the hill and along the valley slopes that quickly speeds up at as much as 3 to 4 m s^{-1} at the upper part of the valley by 1145 LST (see Figure 4b). The anabatic/up valley winds that appear laminar get turbulent as heating peaks and vigorous atmospheric convections dominate the atmospheric boundary layer after 1145 LST. Till these hours local thermal generated wind appears dominant in the valley. However, after around 1330 LST, Figure 4c shows a high-speed southwesterly/southeasterly plain-to-mountain wind of around 6 - 7 m s^{-1} starts approaching the valley from the southern region of the study domain (D3). As southwesterly winds pass through rather narrow neighboring valleys like Waling-Putalibazar leading to Pokhara (see Figure 1 for location), they encounter the southern hill range.

Similarly, the winds passing through the Shukla-Gandaki Valley and southeastern pass of Kotre of the Pokhara Valley arrange as up-valley wind. Interestingly, the southwesterly through Waling-Putalibazar and the up-valley converge inside the Pokhara Valley along its axis (see Figure 4d) in the evening as early as 1730 LST. By 1830 LST, while the up-valley wind is weakened and is replaced by the northeasterly downslope/drainage wind of 2–5 m s^{-1} from between Parche and Namarjung hills, the convergence with southwesterly is stronger possibly generating updrafts in the region of convergence. The convergence lasts for about an hour and a half until the southwesterly plain to mountain wind is weak and the northeasterly wind is dominant that remains active till 2200 LST covering the eastern part of the valley. By 2300 LST, the northwesterly down valley wind along the valley axis initiates making anticlockwise circulation and accumulates cold air in the valley forming a cool air pool the same as the previous night hours.

Condition for the formation of hydraulic jump

In this subsection, some of the wind characteristics and atmospheric stability over the Pokhara valley are highlighted based on the previous subsection to justify the generation of high-speed downslope wind over the southwestern hills like Deurali-Mattikhan of the Pokhara Valley and thus, hydraulic jump in the valley during the early evening.

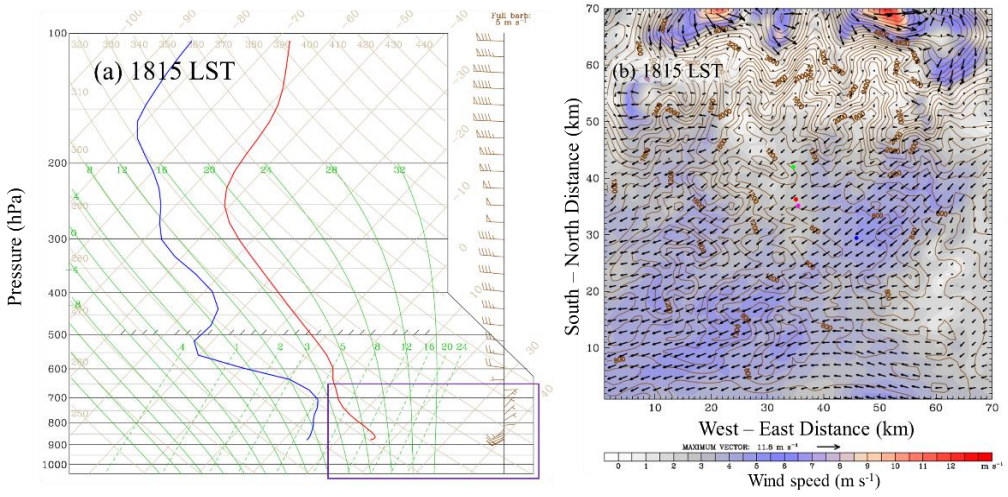

Fig. 5: (a) Skew-T plot showing vertical temperature profile at the top of Deurali-Mattikhan hill top at 1815 LST and (b) spatial distribution of wind (vectors) and wind speed (colored contours) at 2.8 km AMSL at the same time.

The vertical temperature profile at the Deurali-Mattikhan hilltop at 1815 LST in Figure 5a shows the presence of a stable atmosphere as indicated by the presence of a shallow layer of temperature inversion. In addition, a reverse northeasterly flow of around 3 to 5 m s^{-1} at 2.8 km AMSL prevails during the time as seen in Figure 5b, the wind barbs inside the boxed region in Figure 5a, and vertical cross-section plots in Figure 6. Durran (2003) suggests that the presence of a stable layer at the

mountaintop and/or a mean critical level with reverse flow above the level in the middle troposphere enforces upstream flows to the lee downslope storm/wind converting to a supercritical flow. As the southwesterly plain to mountain wind passing through the Waling-Putalibazar area crosses the Deurali-Mattikhan hill range, due to the stable atmosphere and reverse flow above, the southwesterly attains strong downslope wind of more than 6 m s^{-1} in supercritical range at the mountain top and in the lee slope. Figures 6b-g show that the fluid layer in the lee slope is squeezed with a significant downward vertical wind component of 0.5 – 1 m s^{-1}.

Similarly, in the spatial distribution of wind in Figures 4d and 4e, the horizontal wind appears increased in the lee slope region. As this supercritical flow advances in the valley floor, the front head converges with the valley wind at 1730 LST that gradually is replaced by a rather high-speed northeasterly katabatic/drainage wind giving a head-on collision along the valley axis and possibly enhancing the hydraulic jump as explained earlier. This convergence is like the warm northwesterly and cooler southwesterly convergence in the Kathmandu valley (Regmi *et al*. 2003, 2018) except for the fact that the two wind systems appear to suffer direct head-on convergence in the Pokhara Valley. The convergence in the Kathmandu valley is accompanied by a hydraulic jump. Checking the cross-section along line AB in Figure 4f reveals a supercritical flow with squeezed fluid layer on the lee slope and inflation of the layer in the valley floor. To justify quantitatively if the flow is a hydraulic jump the internal Froude numbers are analyzed and described in the following section.

Sectional evaluation of Froude number

In this subsection, we will make a systematic analysis of the cross-sectional behavior of the wind flow, and the Froude number along the cross-section to identify the hydraulic jump-like flow behavior of the southwesterly plain-to-mountain in the Pokhara Valley.

To examine the situation of the southwesterly flow downstream, Froude numbers were calculated at each km along the cross section from Mattikhan hilltop to 10 km away, from 1745 to 1845 LST (see a lifted x-axis (D) from x=14 to 24 km in Figure 6b-f). A systematic examination of Fr along the cross section in Figure 6a shows that the value of Fr increases down the lee slope becoming maximum at around x = 16 or 17 km (D = 2 or 3 km) in the figure where the lee slope is maximum. The flow is supercritical ($Fr > 1$) from 1745 to 1830 LST over the lee slope. However, as the slope decreases the Fr gradually decreases becoming < 1 downstream. Thus, a clear transition of supercritical flow to subcritical flow could be seen in the lee region justifying the occurrences of hydraulic jump in the region from around 1730 LST to 1830 LST. It is notable that the jump region i.e. the critical flow region shifts from around x = 18.5 km (D = 4.5 km) at 1745 to x = 16.5 km (D = 2.5 km) at 1830 LST. The location of the jump is marked by a vertical arrow in the lifted axis in the vertical cross-section plots (see Figure 6b–e). It is interesting to note that the in/above the region of jump mild reverse roller could be seen marked by a dash line oval in Figures 6b–g, not much reported in contemporary studies in the region. The roller appears to form between leeward southwesterly, updraft in the valley, and the reverse flow above. The roller subsequently squeezes as the updraft in the valley shifts west i.e. closer to the lee slope and disappears by 1845 LST in absence of a hydraulic jump. The updrafts of vertical speeds as much as 0.4 to 0.8 m s^{-1} are formed by the convergence of the southwesterly with southeasterly valley wind till 1800 LST and with northeasterly katabatic/drainage wind after 1815 LST, as mentioned in the previous subsection.

The existence of reverse rollers above the hydraulic jump region has been well realized in open channel liquid flows like open streams and has been known to be highly turbulent and hazardous. Rotunno and Bryan (2018) in their idealized simulation showed the existence of such reverse rollers and their turbulent nature in the atmosphere during the hydraulic jump. Though for this day the roller is mild and does not appear much turbulent, the existence of turbulent ones during high winds may not be ignored that may pose substantial threats to aviation activities in the region.

In addition, a similar vertical rotor formation but in a clockwise direction could also be seen in the northeastern edge of the valley as early as 1745 LST due to the interaction of southwesterly and northeasterly katabatic flow (see solid line oval in Figure 6b – 6f). For example, mild rotor formation is seen around x=35 km, 32 km, 25 km, 24 km, and 24 km at 1800, 1815, 1830, and 1845 LST marked by a higher value of turbulent kinetic energy (TKE). Figures 6e and 6f show that during the time, southwesterly flow after the jump overrides the

reverse northeasterly katabatic wind forming the rotor where the TKE of the atmosphere is as much as 0.6 J kg^{-1} at 1830 LST (see Figure 6g). The situation is like a laboratory experiment of the interaction of flows with two different densities. The one with lesser density rides the higher-density fluid where the boundary of the two fluids generates maximum turbulence.

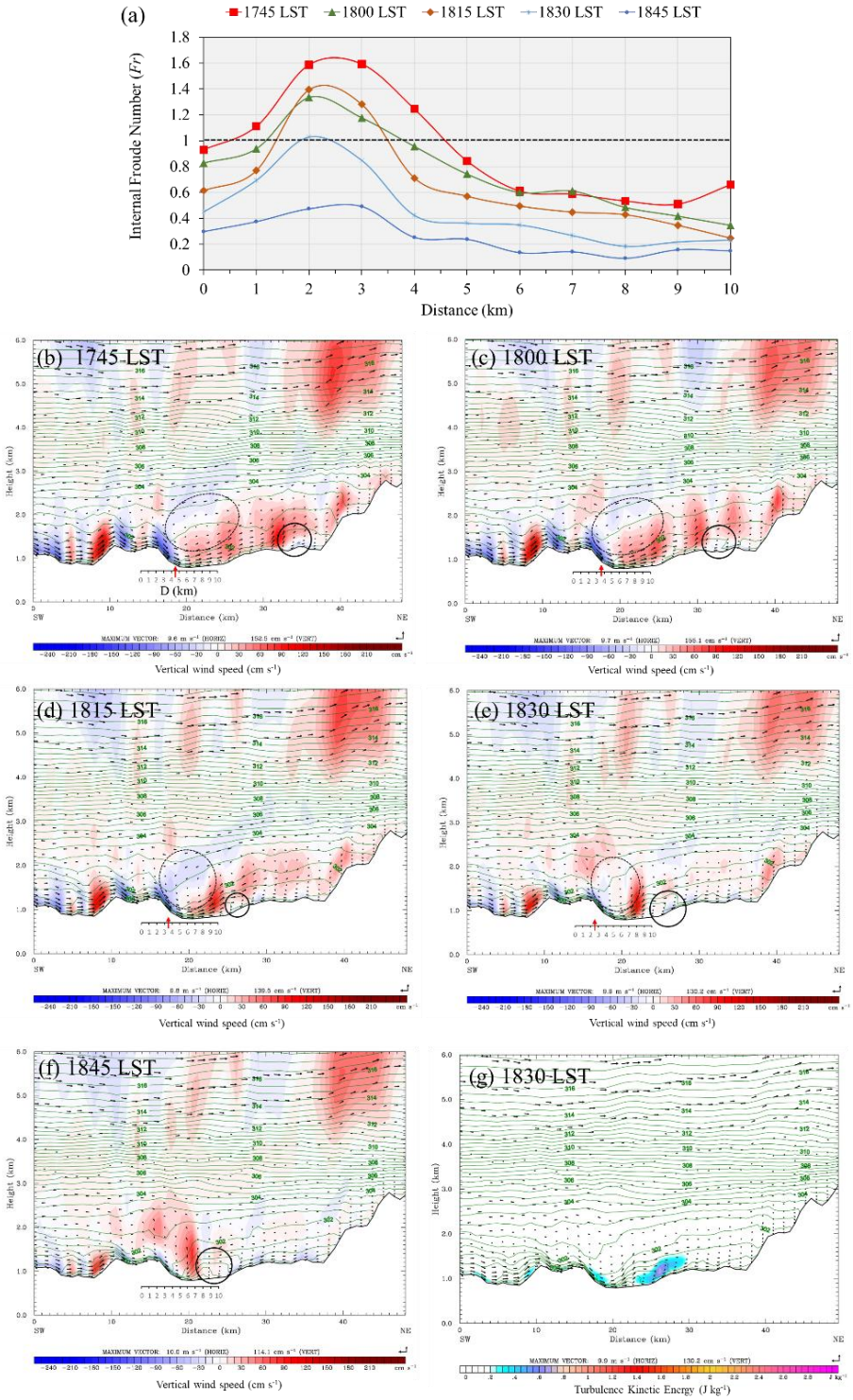

Fig. 6: (a) Distribution of Froude number along the line CD in Figure 4f from 1745 to 1845 LST, and (b-f) vertical cross section of wind (vector), vertical wind speed (colored contour) and potential temperature (line contour) along the line AB in Figure 4f. Dash line oval and solid line oval represents the location of reverse roller and rotor formation, respectively, mentioned in text.

These kinds of rotor formations are critically hazardous for aircraft safety, particularly for the paraglider and parachuting, while the hydraulic jumps of these intensities are equally hazardous for small and light civil aircraft. Since many light aircraft flies to mountainous regions like Mustang from the Pokhara airports, the safety of such aircraft in the valley during Landing and Take Offs needs the consideration of hydraulic jumps.

With the numerical simulations, the detailed characteristic of seasonal activities could be understood and real-time occurrences of such phenomena could be predicted days/hours earlier. Early prediction of possible wind hazards at high spatiotemporal resolutions are highly desired to make aviation activities in the region safer for civil aviation.

CONCLUSION

The Pokhara Valley and its domestic airport have records of a significant number of aviation fatalities involving regular parachute/paragliding accidents, and small and medium aircraft accidents inside and around the region like the recent case of the Yeti aircraft accident on 15 January 2023. With the inauguration of the international airport, the valley is on its way to becoming the nation's second aviation hub. The air traffic of the very light, small, and medium air carriers is expected to be denser in near future in the region. Considering the extreme topographic complexities and associated wind/weather hazards, knowledge of wind systems, atmospheric turbulence, and other wind hazards is necessary, particularly during landing and take-offs. The numerical simulations around the Pokhara Valley during winter have shown hydraulic jump-like flow in the region covering both the domestic and newly opened international airports that could be potentially dangerous for them. It is seen in this study that the regional southwesterly plain-to-mountain wind intruding from the Putalibazar Valley suffers hydraulic jump-like flow with reverse roller during the late afternoon and early evening. The jump is accompanied by the convergence of the southwesterly with southeasterly valley wind and then with the reverse north easterly katabatic/drainage wind. The point of critical layer/jump shifts closer to the lee slope as the northeasterly dominates and the southwesterly weakens. The convergence leads to strong mechanical updrafts of as much as 0.4 to 0.8 m s^{-1} and the southwesterly rides the northwesterly that generates vertical rotor and high turbulence in the boundary between the two layers. The structured network of ground weather observations and extensive study of seasonal characteristics of such phenomena would be necessary to ensure safe aviation in the region.

ACKNOWLEDGEMENT

This study is supported by the University Grants Commission, Nepal under Collaborative Research Grant CRG–75/76–S&T–1 and the Fellowship and research grant Ph.D.-75/76-S&T-17 to Mr. S. Shrestha for his Ph.D. We would like to acknowledge the Department of Hydrology and Meteorology, Ministry of Energy, Water, and Irrigation, Government of Nepal for making AWS data available for validation of the simulation output.

REFERENCES

[1] CAAN (2023a). https://twitter.com/hello_CAANepal/status/1614626415630241794/photo/1

[2] CAAN (2023b). https://twitter.com/hello_CAANepal/status/1614970672320765958/photo/1

[3] Chen, F.; Dudhia, J. Coupling an advanced land surface–hydrology model with the Penn State–NCAR MM5 modeling system. Part I: Model implementation and sensitivity. *Monthly weather review*, **129** (4): 569-585 (2001).

[4] Collier, E.; Immerzeel, W. W. High-resolution modeling of atmospheric dynamics in the Nepalese Himalaya. *Journal of Geophysical Research: Atmospheres*, **120** (19): 9882-9896 (2015).

[5] Dudhia, J. Numerical study of convection observed during the winter monsoon experiment using a mesoscale two-dimensional model. *Journal of Atmospheric Sciences*, **46** (20): 3077-3107 (1989).

[6] Durran, D. R. Downslope winds. *Encyclopedia of atmospheric sciences*, 644-650 (2003).

[7] Himalisanchar (2022). https://himalsanchar.com/17-people-died-in-paragliding-accidents-in-26-years/

[8] Janjic´, Z. I. Nonsingular implementation of the Mellor–Yamada level 2.5 scheme in the NCEP Meso model. NCEP Office Note 437 (2001).

[9] Kitada, T.; Regmi, R. P. Dynamics of air pollution transport in late wintertime over Kathmandu Valley, Nepal: As revealed with numerical simulation. *Journal of Applied Meteorology and Climatology*, **42** (12): 1770-1798 (2003).

[10] Lee, J.; Seo, J. M.; Baik, J. J.; Park, S. B.; Han, B. S. A Numerical Study of Windstorms in the Lee of the Taebaek Mountains, South Korea: Characteristics and Generation Mechanisms. *Atmosphere*, **11** (4): 431 (2020).

[11] Mlawer, E. J.; Taubman, S. J.; Brown P. D.; Iacono, M. J.; Clough, S. A. Radiative transfer for inhomogeneous atmospheres: RRTM, a validated correlated-k model for the longwave. *Journal of Geophysical Research: Atmospheres*, **102** (D14): 16663-16682 (1997).

[12] Norris, J.; Carvalho, L. M.; Jones, C.; Cannon, F. WRF simulations of two extreme snowfall events associated with contrasting extratropical cyclones over the western and central Himalaya. *Journal of Geophysical Research: Atmospheres*, **120** (8): 3114-3138 (2015).

[13] Panday, A. K.; Prinn, R. G.; Schär, C. Diurnal cycle of air pollution in the Kathmandu Valley, Nepal: 2. Modeling results. *Journal of Geophysical Research: Atmospheres*, **114** (D21) (2009).

[14] Peña, A.; Santos, P. Lidar observations and numerical simulations of an atmospheric hydraulic jump and mountain waves. *Journal of Geophysical Research: Atmospheres*, **126** (4): e2020JD033744 (2021).

[15] Regmi, G.; Shrestha, S.; Maharjan, S.; Khadka, A. K.; Regmi, R. P.; Chandra Kaphle, G. The Weather Hazards Associated with the US-Bangla Aircraft Accident at the Tribhuvan International Airport, Nepal. *Weather and Forecasting*, **35** (5): 1891-1912 (2020).

[16] Regmi, R. P. Aviation hazards over the Jomsom Airport of Nepal as revealed by numerical simulation of local flows. *Journal of Institute of Science and Technology*, **19** (1): 111-120 (2014).

[17] Regmi, R. P.; Maharjan, S. Wind Energy Potential of Middle Hills of Nepal Himalaya. *World Wind Energy International Quarterly Bulletin* 1 (2013).

[18] Regmi, R. P.; Kitada, T.; Kurata, G. Numerical simulation of late wintertime local flows in Kathmandu valley, Nepal: Implication for air pollution transport. *Journal of Applied Meteorology and Climatology*, **42** (3): 389-403 (2003).

[19] Regmi, R. P.; Kitada, T.; Dudhia, J.; Maharjan, S. Large-scale gravity current over the middle hills of the Nepal Himalaya: Implications for aircraft accidents. *Journal of Applied Meteorology and Climatology*, **56** (2): 371-390 (2017).

[20] Regmi, R. P.; Kitada, T.; Maharjan, S.; Shrestha, S.; Shrestha, S.; Regmi, G. Wintertime boundary layer evolution and air pollution potential over the Kathmandu Valley, Nepal. *Journal of Geophysical Research: Atmospheres*, **124** (8): 4299-4325 (2019).

[21] Rotunno, R.; Bryan, G. H. Numerical simulations of two-layer flow past topography. Part I: The leeside hydraulic jump. *Journal of the Atmospheric Sciences*, **75** (4): 1231-1241 (2018).

[22] Skamarock, W. C.; Klemp, J. B.; Dudhia, J.; Gill, D. O.; Liu, Z.; Berner, J.; Wang, W.; Powers, J. G.; Duda, M. G.; Barker, D. M.; Huang, X. Y. *A Description of the Advanced Research WRF Model Version 4*. National Center for Atmospheric Research: Boulder, CO, USA (2019).

[23] Thompson, G.; Rasmussen, R. M.; Manning, K. Explicit forecasts of winter precipitation using an improved bulk microphysics scheme. Part I: Description and sensitivity analysis. *Monthly Weather Review*, **132** (2): 519-542 (2004).

[24] Whiteman, C. D. *Mountain meteorology: fundamentals and applications*. Oxford University Press (2000).